

Scaling effects for Compression Loaded of Corrugated-core Sandwich Panels

M.R.M.Rejab^a, N.Z.M. Zaid, J.P. Siregar and D. Bachtiar

Faculty of Mechanical Engineering, Universiti Malaysia Pahang, 26600 Pekan, Pahang, Malaysia

^aruzaimi@ump.edu.my

Keywords: Corrugated-core sandwich panels, Compression Strength, Aluminum Alloy, Composites, Fracture Modes

Abstract. The compressive responses and failure investigations of corrugated-core sandwich panels subjected to lateral compression are presented. The results of finite element (FE) analysis using Abaqus are compared with experimental results from tests on sandwich panels based on corrugations of aluminum alloy, glass fibre-reinforced plastic (GFRP) and carbon fibre-reinforced plastic (CFRP). Particular focus is placed on identifying the scaling effects of number of unit cells and the thickness of the cell walls in dominating the overall deformation and local collapse of the panel. The effect of increasing the number of unit cells, cell wall thickness, specimen's width and deformation behaviour are investigated. The FE predictions have been shown to in reasonably agreement with the experimental measurements. The evidence suggests that corrugated composite cores offer significant potential as lightweight cores materials in sandwich construction.

INTRODUCTION

Sandwich structures with fibre reinforced plastic skins and a cellular core have proven superior weight specific stiffness and strength properties compared to its monolithic counterpart. In recent years, many researchers have proposed various core designs with an improved quasi-static and dynamic performance and these comprise of various polymeric and aluminium foams [1], metallic trusses [2-4], honeycomb cores [5-6] (square, hexagonal, triangular) and prismatic cores [7-8] (diamond lattice and corrugations).

Polymeric foams and honeycomb structures are commonly being used as core materials. For a more lightweight material, honeycomb core structures made from aluminium or Nomex® aramid paper are leading candidates when it comes to weight-specific mechanical properties. However, honeycomb sandwich structures, especially in aircraft applications suffer from drawbacks such as humidity retention in the closed cells [9].

Recently, many researchers on the advanced cellular core design projects have investigated and proposed alternatives to the honeycomb core such as the folded core structure, and its experimentally proven in solving the problem of humidity accumulation in closed cell sandwich core materials and these structures have multifunction properties [10,11]. Researchers have also looked at the other alternative ways to use corrugated cores in sandwich panels [12,13]. Generally, corrugated cores have been used over many decades in civil, naval, automotive and aerospace applications i.e.: corrugated roofs made from metal; cardboard sandwich cores used for packaging [14-15]. For extreme loading, corrugated metal sandwich cores have been shown to offer excellent shock resistant properties, mainly due to their high longitudinal stretching and shear strength [16].

CORRUGATED-CORE SANDWICH PANELS

The focus of this paper is to study the effect of increasing the number of unit cells, the cell wall thickness and the deformation behaviour that differ to the material properties. Three types of material have been used in the study, which are aluminium alloy 2024-O (AL), a fabric-type glass fibre reinforced plastic (GFRP), and a woven carbon fibre reinforced plastic (CFRP). Plates of corrugated-core were prepared using special triangular profile of 45° with a 210mm by 240mm

effective area of fabrication. Figure 1 shows the mould which was made from mild steel with a nominal 10mm height and 20mm length for each of the unit cell designs. The choice of the 45° of corrugation angle was because of it gives an optimum shear modulus with respect to stretching and bending stiffness of the monolithic core member [12].

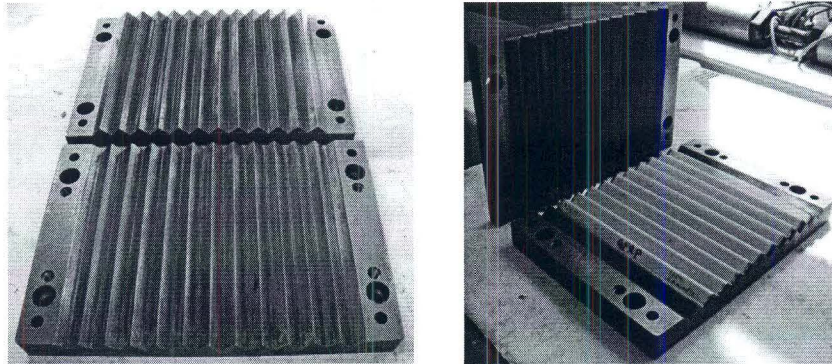


Figure 1: Photograph of the corrugated mould.

During fabrication, the material was placed between the upper and lower moulds, and then manufactured using a hot press machine according to the manufacturer's recommended processing cycle. After curing, the sample was removed from the mould and visually inspected for any defects, once the hot press had cooled to a temperature below 60°C.

Next, the core was bonded between the two skins using strong epoxy adhesive (Araldite 420 A/B). The sandwich structure was then heated in an oven at a temperature of 120°C for about 1 hour, to cure the adhesive. Following this, the structure was cut into test sample with dimensions; 100mm length and 25mm width.

Figure 2 shows the corrugated-core sample consisting of repetitions of an identical unit cell. The consistency of the dimensions of every single unit cell after the fabrication process is clearly critical. An exact measurement and invariable identity of unit cell are to ensure the reliability of the repeated of experimental results.

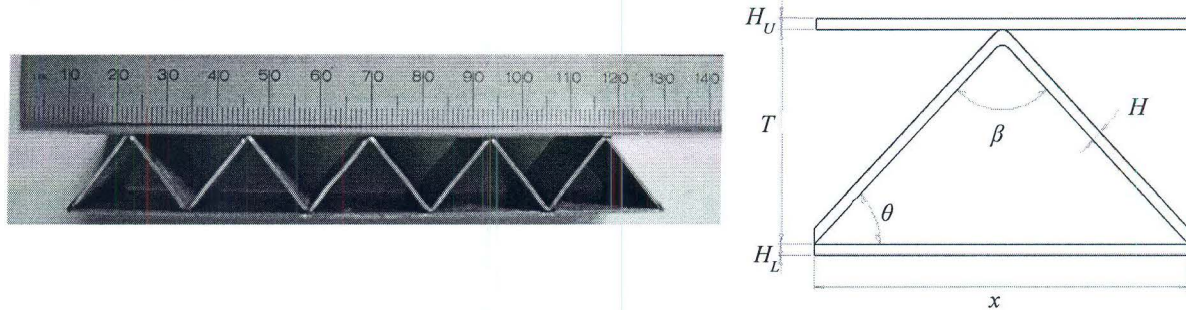


Figure 2: Geometry of corrugated-core sandwich panel.

Generally, the unit cell is based on a triangular profile. The geometric parameters plotted in Figure 2 are annotated as follows: θ and β are the internal angle of a unit cell for the corrugated-core sandwich panel; T is the height of the core; H_U and H_L are the upper and lower thickness of the skins, respectively; H is the average thickness of inclined core members and also called as wall thickness; x is the length of the core; and w is the width of a sample. Due to the predetermined mould design, the value of x is 20mm length while θ and β are set to be 45° and 90°, respectively. For preparation of the test specimens, the value of width was consistently cut into 25mm. And then, five different numbers of corrugated cores have been cut according to the size of unit cells.

EXPERIMENTAL WORK

Compression tests on the corrugated-core sandwich panels were conducted using an Instron series 4505 testing machine. All the test specimens were prepared in a rectangular form, based on the different number of unit cells and thickness.

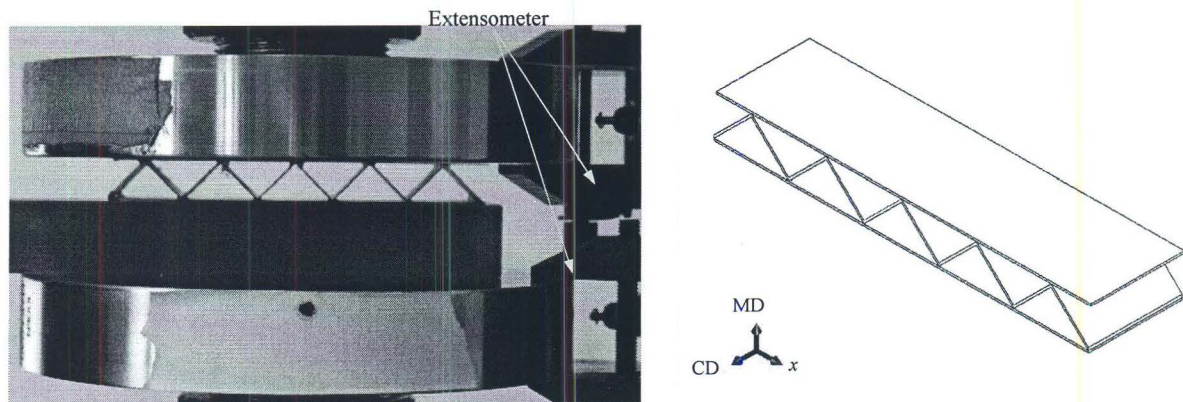


Figure 3: Compression testing setup with the displacement measurement system.

Figure 3 shows the specimen placed between the platens of the machine where it was deformed by applying a uniform lateral compression at a static loading rate of 1mm/minute. As the main area of interest was in the deformation behaviour of the panels, an extensometer was used to gather strain data. The load-displacement trace was recorded until the specimen was entirely crushed. The experiments showed that there exists a fundamental difference in the behaviour of the different panels.

Aluminium Alloy Corrugated-Core

A typical load-displacement trace for AL corrugated-core sandwich panel is presented in Figure 4. The deformed configurations of this ductile specimen, corresponding to various levels of the prescribed displacement as marked on the curve, have been recorded by high speed video camera.

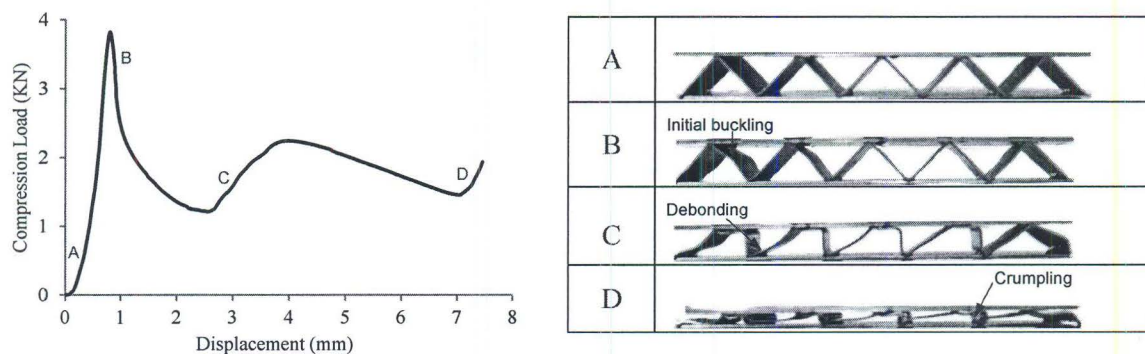


Figure 4: Typical load-displacement trace with damage development in an AL corrugated-core sandwich panel with five unit cells.

Upon loading, the specimen shows a nonlinear response during the early loading stage. This may partly be attributed to the machine compliance and, perhaps more significantly, to the fact that closer inspection revealed that both skins were not parallel to each other. As the result, the initial deformation of the panel is influenced by the flattening of these skins. After this initial “stiffening”, the specimen then responds linearly up (as in point A) to the first peak in the load, and the

deformation was symmetrical about the axis of loading. After reaching the first peak load, one of the struts in the corrugated-core was partially bent, the overall stiffness of the specimen then decreased, the load required to further deform the panel gradually decreases due to the propagation of localised buckling in the corrugated-core. The response then becomes progressively nonlinear (point B). This is followed by a sudden drop in the applied load as the panel loses stability due to plastic buckling. At the point C, the corrugated-core takes on a trapezium shape, and the applied load increases due to the interaction between the surfaces of the deformed struts and the flat skins. Finally, point D shows the corrugated-core is completely densified, where both the skins and corrugated-core are flattened and in some cases the sides of edge are debonding. Figure 5 show the linear relationship between the compression strength and stiffness to the number of unit cells for specimens with $H=0.53\text{mm}$.

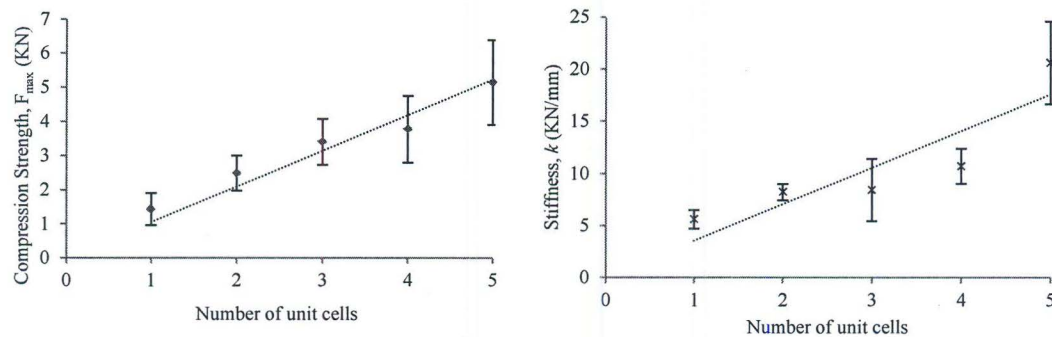


Figure 5: Compression strength and stiffness responses to number of unit cells of AL corrugated-core sandwich panels, $H = 0.53\text{mm}$.

Glass Fibre-Reinforced Plastic

GFRP corrugated-core sandwich panel shows brittle behaviour of material crushing under compression load as seen in Figure 6.

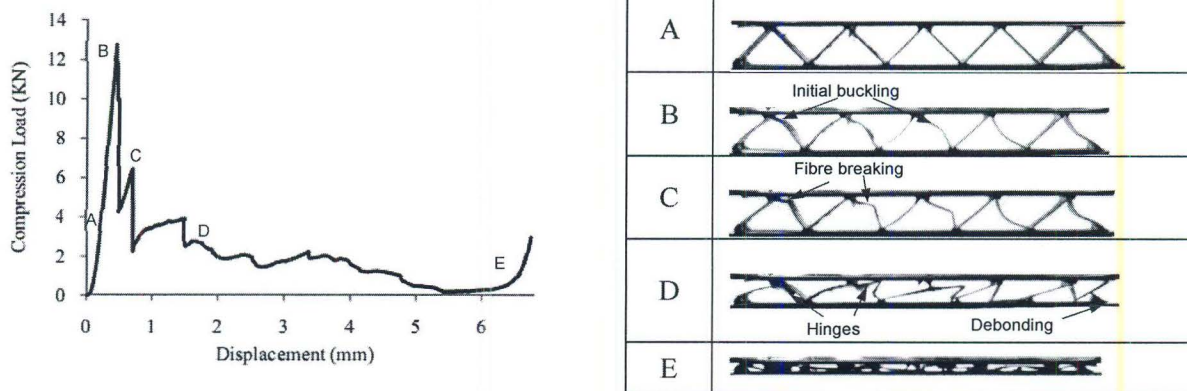


Figure 6: Typical load-displacement trace with damage development in five unit cells of GFRP corrugated-core sandwich panel.

At the point B, initial cell wall buckling was visible followed by a compression fracture at the peak load. The drop in the load-displacement diagram is steeper than in the AL sample due to the different failure mechanisms involved (points C to D): a formation of hinges in the middle of the cell wall after fibre breaking, debonding of the adhesive between the surfaces and continuous crushing after failure at the cell wall from the upper to lower skins. Finally, at point E the corrugated-core is completely crushed, where both the skins and the core are flattened.

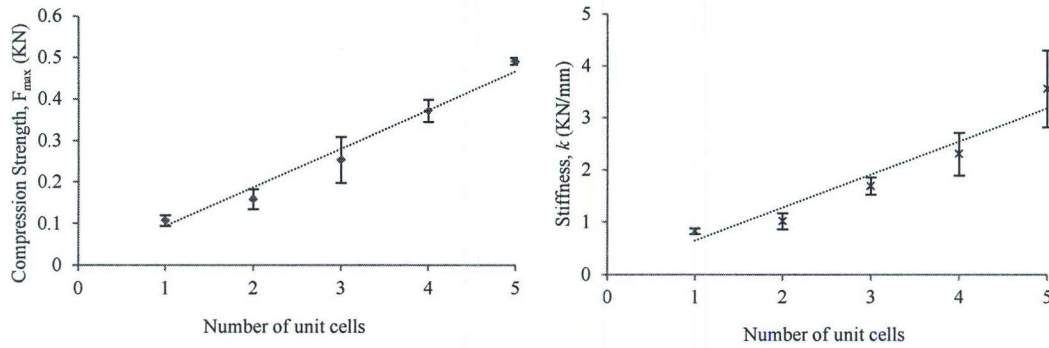


Figure 7: Compression strength and stiffness responses to number of unit cells of GFRP corrugated-core sandwich panels, with an average $H = 0.17\text{mm}$.

In Figure 7, the experimental data of the specimens with an average $H = 0.17\text{mm}$, shows a linear relationship between both the compression strength and stiffness with increasing number of unit cells. While in Figure 8, the scattered experimental data shows a linear relationship between the compression strength and stiffness for different cell wall thicknesses.

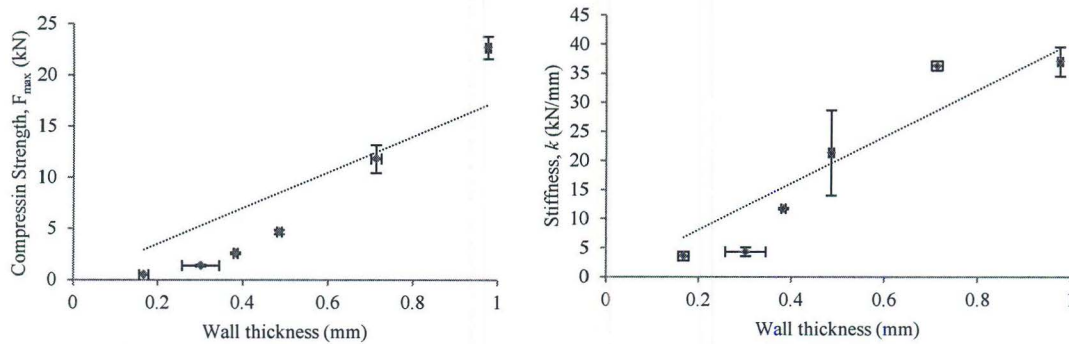


Figure 8: Compression strength and stiffness responses to cell wall thickness of GFRP corrugated-core sandwich panels.

Carbon Fibre-Reinforced Plastic

The failure mechanisms in the CFRP corrugated-core under compression loading are shown in Figure 9.

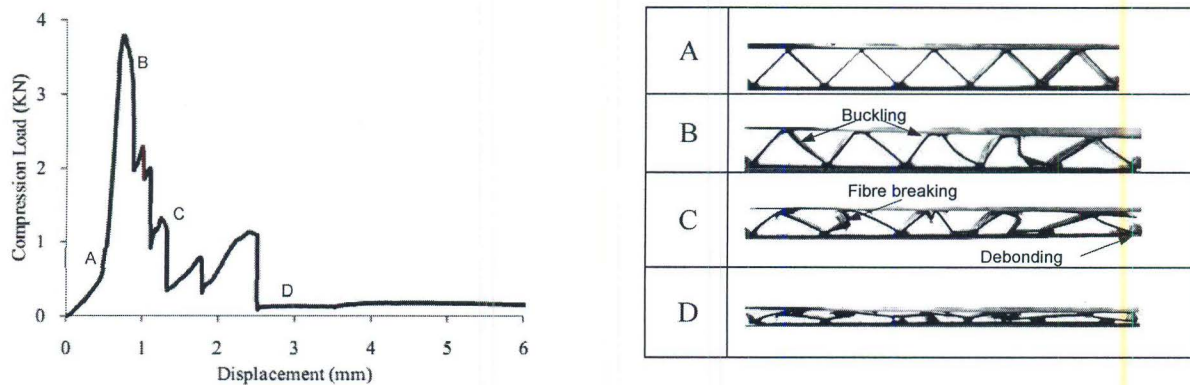


Figure 9: Typical load-displacement trace with damage development in five unit cells of CFRP corrugated-core sandwich panel.

Initial failure was dominated by cell wall buckling before reaching a high stress level. The load-displacement diagram is steeper than that for the AL structure and the post-damage failure modes are similar to the GFRP corrugated-core. In Figure 10, the experimental data of the specimens with an average $H = 0.44\text{mm}$, shows a good linear relationship between the compression strength and stiffness to the number of unit cells.

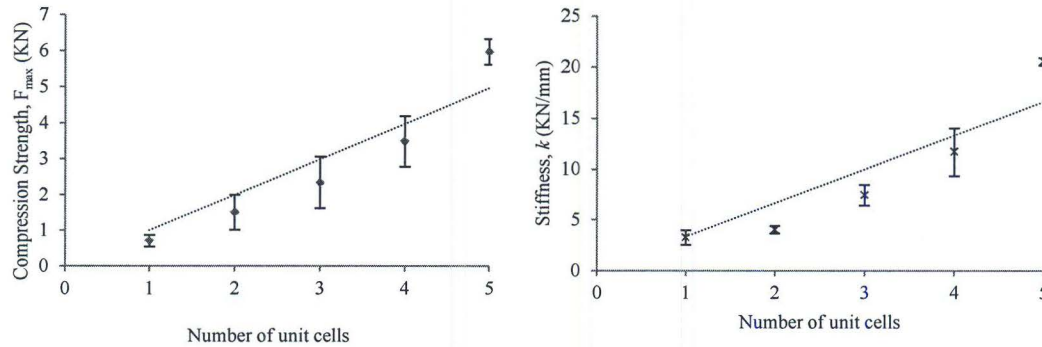


Figure 10: Compression strength and stiffness responses to number of unit cells of CFRP corrugated-core sandwich panels, with average $H = 0.44\text{mm}$.

Meanwhile, the somewhat scattered data in Figure 11 shows a proportional relationship between the compression strength and cell wall thickness. However, for the stiffness response, there is considerable scatter in the data to significant variations in the cell wall thickness, which consequently reduces the rigidity of the strut member.

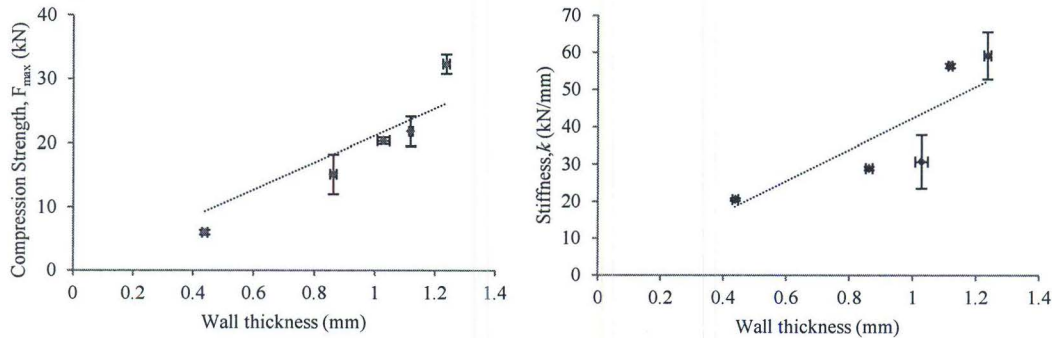


Figure 11: Compression strength and stiffness responses to cell wall thickness of CFRP corrugated-core sandwich panels.

MODELLING AND SIMULATION

The aim of the simulation is to predict the compression strength and stiffness for different types of material, and in the meantime able to reduce experimental efforts where a large number of core geometries can be characterised numerically in the future.

Model Development

A numerical analysis of the corrugated-core sandwich panels under compression loading was performed using the ABAQUS finite element software. It suffices to model five corrugations without the skins, meshed using 3-dimensional linear 4-node shell elements (S4R) where the core and the platen are connected with a contact formulation. All degrees of freedom of the nodes along the upper and lower edges were fully constrained except in U2-direction at the upper edge. Due to imperfection issues (irregular geometry, uneven cell wall thickness, etc), the model was simulated by modifying the mesh elements densities at each struts to simulate closely to 'real experimental behaviour'. As in Figure 12, this approach was able to reduce the overstiffness reaction from the effect of geometrical imperfection in the cell wall structures. For ductile materials, an isotropic

hardening model with an uniaxial true stress versus logarithmic plastic strain was tabulated as input property whereas for brittle material, Hashin's damage model was used to predict the behaviour of the composites.





No.	Simulation	Experiment
Model		
Initial buckle		

Figure 12: Modelling of corrugated-core with comparing to initial failure behaviour.

Simulation Results

Figure 13 shows a comparison between the FE analysis and experimental results for the AL, GFRP and CFRP corrugated-core sandwich panels.

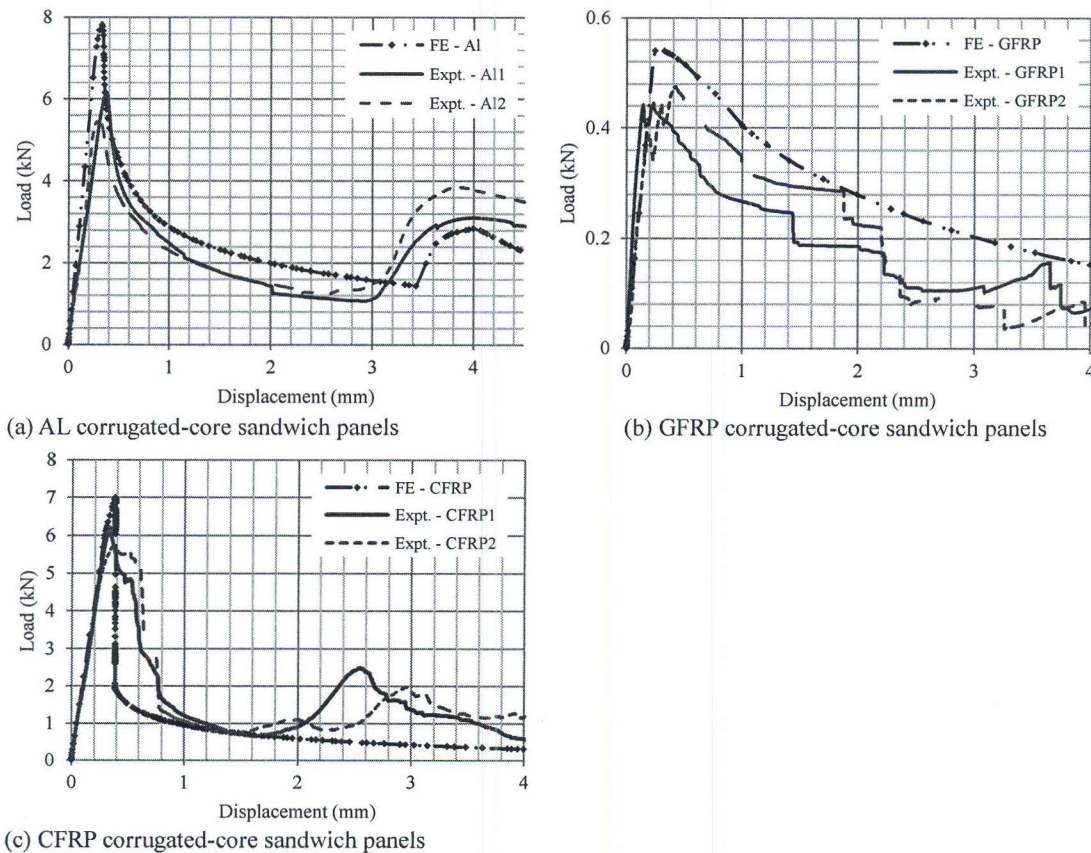


Figure 13: The FE simulation shows a good agreement with experimental results; (a) AL with $H = 0.53\text{mm}$, (b) 2 plies of GFRP with $H = 0.16\text{mm}$, (c) 2 plies of CFRP with $H = 0.44\text{mm}$.

The peak load is higher in the simulations than in the two experiments, however the load-displacement curve indicates a high degree of agreement in the stiffness characteristics and collapse

behaviour, which is dominated by buckling. The cell wall collapse in the experiments and simulation occurs at similar displacement values. The corrugated-core observed within the experiments tended to form sharp buckle, whereas the corrugated-core in the simulation buckled in a sinusoidal shape. However, the overall buckling pattern in the simulation model agrees very well to the experiments.

CONCLUSIONS

The compressive responses and failure mechanisms of corrugated-core sandwich panels with three different materials subjected to uniform lateral compression were explained both in experimental and simulation works. The following conclusions are made:

- a. From the observations, it found that initial failure in the structures was dominated by the instability of the struts when cell wall starts to buckle.
- b. A linear relationship between the compression strength and stiffness of the materials to the number of unit cells and cell wall thicknesses.
- c. Simulation of the panel showed that not only numerous modelling parameters and an appropriate material model for the cell wall influence the simulation result, also the consideration of imperfection is critical.
- d. With the potential of parametric models and the ability to cover the stiffness and strength of the respective corrugated-cores with an acceptable degree of accuracy, a geometry optimisation can be performed in order to identify a corrugated-core with optimised mechanical properties with a minimum density.

This paper only covers the lateral compression behaviour but this investigation would be extended to transverse shear properties using Arcan testing technique and the behaviour of corrugated-core panels under various dynamic loadings.

ACKNOWLEDGEMENTS

The authors are grateful to the Ministry of Education for funding this research (FRGS/1/2014/TK01/UMP/02/3).

REFERENCES

- [1] D.D. Radford, G.J. McShane, V.S. Deshpande and N.A. Fleck: *Int. J. Solid Struct.* Vol. 43 (2006), p.2243
- [2] G.W. Kooistra, V.S. Deshpande and H.N.G. Wadley: *Acta Mater.* Vol. 52 (2004), p.4229
- [3] V.S. Deshpande and N.A. Fleck: *Int. J. Solid Struct.* Vol. 38 (2001), p.6275
- [4] G.J. McShane, D.D. Radford, V.S. Deshpande and N.A. Fleck: *Eur. J. Mech.* Vol. 25(2) (2006), p.215
- [5] S. Lee, F. Barthelat, J.W. Hutchinson and H.D. Espinosa: *Int. J. Plasticity* Vol. 22(11) (2006), p.2118
- [6] F. Côté, V.S. Deshpande, N.A. Fleck and A.G. Evans: *Mater. Sci. Eng. A* Vol. 380 (2004), p.272
- [7] M.T. Tilbrook, D.D. Radford, V.S. Deshpande and N.A. Fleck: *Int. J. Solids Struct.* Vol. 44(8) (2007), p.6101
- [8] F. Côté, V.S. Deshpande, N.A. Fleck and A.G. Evans: *Int. J. Solid Struct.* Vol. 43 (2006), p.6220
- [9] A.S. Herrmann, P.C. Zahlen and I. Zuardy: *Sandwich Structures* Vol. 7 (2005), p.13
- [10] G.V. Movchan: *Russian Aeronautics* Vol. 50 (2007), p.439
- [11] S. Fisher, K. Drechsler, S. Kilchert and A. Johnson: *Composites: Part A* Vol. 40 (2009), p.1941
- [12] D. Zenkert and S. Kazemahvazi, *Composites Sci. and Tech.* Vol. 69 (2009), p.913
- [13] D. Zenkert, S. Kazemahvazi and D. Tanner: *Composites Sci. and Tech.* Vol. 69 (2009), p.920
- [14] T.J. Lu, C. Chen and G. Zhu: *J. of Composite Materials* Vol. 25 (2001), p.2098
- [15] Z. Aboura, N. Talbi, S. Allaoui and M.L. Benzeggagh: *Composite Struct.* Vol. 63 (2004), p.53
- [16] N.A. Fleck and V.S. Deshpande: *J. Appl. Mech.* Vol. 71 (2004), p.386